scientific reports

Check for updates

OPEN

Investigation on micro drilling of low carbon NiTi alloy using tungsten carbide micro drill tool

M. Adam Khan[1], G. Ebenezer[1], J. T. Winowlin Jappes[1], Abdel-Hamid Ismail Mourad[2,3]✉ & Dinu Thomas Thekkuden[4]

The demand for advancements in Functional Materials due to their extensive applications especially on the development of product miniaturization is ever growing. The current study focusses on the influence of micro drilling process parameters such as tool rotational speed (1500, 2000, 2500 rpm), feed rate (0.2, 0.4, 0.6 mm/min) for a constant length of cut (500 µm) with 495 µm diameter drill tool on the low carbon nickel-titanium (NiTi) alloy, augmented with 0.05 wt% carbon. Studies on the selected rotational speeds and 0.05% carbon added NiTi are highly lacking. A blind hole of 500 µm was micro drilled on NiTi alloy using tungsten carbide (WC) micro drill bit. The results have revealed that high-speed machining at 2500 RPM facilitated the production of an accurately drilled hole with a close dimension of 501 µm at a minimum feed rate (0.2 mm/min). Under the same high-speed conditions, an increase in feed rate leads to a larger drill hole diameter due to tool outing losing precision. In addition, the drill tool experiences buckling as the feed rate increases, drill opening with pre-eminent plastic deformation, and shear, ultimately momentous in the formation of metal chips. In terms of machining time, high-speed machining requires less time (0.43 min) to complete the drilling process, whereas slow-speed machining consumes more time (up to 1.78 min). In high-speed machining, the tool edges undergo severe wear, characterized by both adhesion and abrasion. This work introduces optimized procedure to produce micro sized holes through high-speed machining of low-carbon NiTi alloy using a WC drill tool.

Keywords Micro drilling, WC drill tool, NiTi alloy, Tool wear, Machining time

Micromachining has emerged as a dynamic frontier in the manufacturing sector, known for its capability to intricately craft components on a remarkably small scale. Recognized as a pivotal manufacturing technique, micromachining is experiencing heightened demand across a spectrum of industries. Its proficiency in producing precision-driven miniature structures has positioned it at the forefront of technological progress. The increasing emphasis on miniaturization in electronics, medical devices, and aerospace has driven a growing need for micromachining, enabling the development of components with dimensions measured in micrometres. As industries continually expand the possibilities at the microscale, the versatility and cost-effectiveness of micromachining have become integral for shaping innovative solutions, thereby cementing its role as a crucial player in the evolution of contemporary manufacturing. In the current research landscape, the demand for functional materials in applications such as micro-robots, biomedical implants, nuclear reactor shields, and automotive components continues to flourish[1–3]. The current research focusses on the Nickel-Titanium (NiTi) alloy having wide applications in biomedical devices such as stents, catheters, guide wires, orthopaedic and dental implants and drug delivery systems whereas actuators, sensors, micro valves and micro pumps made of NiTi are getting popular and demanded. Micro machining is necessary for producing micro components; however, the limitation in the size of the components is very challenging. In this context, micro drilling of the prominent shape memory material NiTi using Tungsten carbide micro drill tool has huge industrial significance.

To emphasize more, Nickel-titanium (NiTi) alloy stands out as a highly sought-after material for use in biomedical industries, aerospace components, and aviation engines. This preference is attributed to its superior

[1]Department of Mechanical Engineering and Centre for Surface Engineering, Kalasalingam Academy of Research and Education , Krishnankoil, Tamil Nadu 626126, India. [2]Department of Mechanical and Aerospace Engineering , United Arab Emirates University , P.O. Box 15551, Al-Ain, United Arab Emirates. [3]National Water and Energy Center, United Arab Emirates University, P.O Box 15551, Al Ain, United Arab Emirates. [4]Mechanical and Industrial Engineering Department , Abu Dhabi University , 59911 Abu Dhabi, United Arab Emirates. ✉email: ahmourad@uaeu.ac.ae

mechanical properties and electrochemical stability[4]. Literatures extensively cover the development of nickel and titanium-based alloys, detailing variations, and modifications in alloying elements[5–11]. Various Ni_xTi_y materials with different combinations of alloying elements, including carbon, copper, cobalt, and others, are open for discussion. These materials have been engineered to possess commendable tribological properties, fatigue strength, and super-elastic properties. Recent research has embraced additive manufacturing techniques for the development of NiTi alloy, incorporating modifications in alloying elements[6]. Metal cutting technology stands out as a predominant technique for removing unwanted material. Specifically, biomedical and micro-mechanical systems necessitate highly precise micro-machining processes to drill difficult-to-cut materials.

Szwajka et al.[12] presented the effect of mechanical micro-drilling of Inconel 625 alloy and reported that the drill bit suffered premature breakage due to its fragile nature, resulting in lower tool life. The findings of the research also indicate that micro-mechanical re-drilling effectively rectifies the geometric discrepancies that arise from the initial laser pre-drilling. The sequential mechanical micro-drilling led to an extension in the lifespan of the drill.

Shashank et al.[13] drilled micro holes into the Aluminium 7075-T6 workpiece material employing the pilot hole drilling at a diverse range of spindle speeds and feeds. The radial force and torque divulge a pattern of increase and decrease with drill bit rotational speed, and the same reflects the 'size effect.' The oversize error follows an ascending drift with rotational speed and is closely associated with the variations in radial force and radial torque.

Eren et al.[14] examined the high-speed machining characteristics and phase change characteristics of NiTi shape memory alloy. The findings on tool wear indicate that the Polycrystalline Diamond (PCD) tool exhibits significant potential over carbide, particularly when considering the constraints associated with rapid tool wear in high cutting speed ranges. In comparison to the unprocessed sample, negligible variations in functional properties were observed at the elevated cutting speed of 250 m/min. Likewise, the addition of elements to the base material changes the properties. Kumar et al. showed that the surface modification using silicon powder using wire electric discharge machining was prominent than with aluminium powder. In this study, the 0.05% carbon added to NiTi is considered and therefore a research study on the proposed material is needed[15].

During machining, the formation of burrs is contingent upon the mechanism of tool kinematics and the material's behaviour during the metal cutting process[16]. According to Ramesh and Akinori[17], in the micro-machining of nitinol, the tool and work interface play a pivotal role in determining the process performance, considering material phase conversion. Tool wear rate is a crucial factor in micro-drilling, particularly when drilling tough-to-cut materials. The thrust cutting force generated during micro-drilling significantly contributes to the blunting of the drill tool[18]. Additionally, the nomenclature of the micro-cutting tool also contributes to increasing productivity and extending tool life[19]. In some instances, the surface of the cutting tool is improved using processes such as Physical Vapour Deposition (or) Chemical Vapour Deposition to enhance tool life when machining tough-to-cut materials[20].

Abhishek and Soumya[21] designed an analytical model to evaluate the adequacy or insufficiency of the Minimum Quantity Lubrication (MQL) flow rate for diverse cutting conditions in a micro-drilling process. The model was constructed by taking into account tool geometry, the investigational value of chip thickness, and the material properties of the workpiece. Variations in feed and spindle speed were found to influence the lubrication area. Specifically, in the ploughing region, the necessary lubrication area increased with the feed rate. The quality of the machined surface can be assessed by surface roughness, where the machining parameters such as feed rate and cutting speed highly cause change in the surface roughness[22]. The feed rate along with spark gap voltage, pulse-on time, pulse off-time and wire feed rate in wire spark erosion process significantly affect the surface quality[23].

Hegde et al. developed artificial neural network to predict the NiTi hole quality and thrust force based on mainly tool rotational speed and feed rate, however the rotational speed was high with levels 10,000, 20,000 and 30,000 rpm and feed rate with three levels of 0.075, 0.125, and 0.25 µm/rev[24]. On the other hand, Chaudhary et al. investigated rotational speed (25,000, 37, 500, 50,000 rpm), feed rate (0.15, 0.2, 0.25 mm per min) and tool diameter ranging from 100 to 200 µm where the findings proved diameter of the tool was the significant parameter compared to rotational speed and feed rate for the optimum hole quality of NiTi metal alloy[25]. Matta et al. reported the formation of micro cracks on NiTi alloy at higher rotational speed where the investigated rotational speed were from 10,000 till 30,000 rpm[26]. The above research proves the implication of high-speed process, however lower rotational speed are also preferred for certain applications. For example, Sethi et al. utilized only 500 rpm in addition to pulsing frequency, where pulsing frequency was considered as a parameter affecting the precision of NiTi micro channels[27]. More number of reported findings were based on high rotational speed compared to low rotational speed, and this supports the necessity for investigating the effect of low rotational speed on the accuracy and precision of micro drilling of NiTi. In addition, the literature emphasises more on the Electric Discharge Machining (EDM), Laser Beam Machining (LBM), and Electrochemical Machining (ECM) based process for producing holes and the capability of the conventional drilling process for micro machining has to be further explored. Therefore, the influence of three levels of low rotational speed using the conventional drilling process is explored in the presented research.

Further based on the aforementioned discussions, the micro-drilling using drill emerges as one of the most effective techniques to achieve a competent surface veracity while machining functional/tough-to-cut materials[28–30]. Electric Discharge Machining (EDM), Laser Beam Machining (LBM), Electrochemical Machining (ECM), and more, on materials such as composites, conventional metals, titanium-based alloys, and nickel-based alloys have been explored more recently; however, the potential of micro drilling process for application suitability is to be explored. The glimpse of available work (indicative) in the micro drilling is depicted in Table 1. From Table 1, the literatures have extensively available for the binary NiTi system under the various combinations of Ni and Ti. The ternary compounds are mostly copper, cobalt, hafnium, zirconium, niobium, etc.

S. No	Authors and year	Material	Machining method	Outcomes
1	Takale, A. M., & Chougule, N. K. (2019)[5]	$Ti_{49.4}Ni_{50.6}$	Wire electro discharge machining	Optimized trail run produced fewer micro cracks, low residual stress and less carbon contains on the machines surface
2	Geier, N., Patra, K., Anand, R. S., Ashworth, S., Balázs, B. Z., Lukács, T., & Davim, J. P. (2023)[1]	Glass and carbon fibre reinforced polymer composites	Mechanical micro-drilling	Delamination resulting from micro-drilling is milder compared to that from larger-scale drilling. Geometrical defects are caused by micro-drilling, such as delamination, burrs, and fiber pull-outs, among others.
3	Agrawal, V., Gajrani, K. K., Mote, R. G., Barshilia, H. C., & Joshi, S. S. (2022)[3]	Inconel 718	Mechanical micro-drilling	A theoretical framework is developed to forecast tool wear during drilling over time and to assess the longevity of drills coated with anti-abrasion, TiAlSiN, and TiAlN materials. These coatings extended the lifespan of the drills, with the wear rate being most pronounced at the drill's corner.
4	Soni, H., & MR, R. (2018)[9]	$Ti_{50}Ni_{45}Co_5$	Wire Electro Discharge Machining	The optimum setting through the PCA and GRA gave the settings for higher MRR and lower SR.
5	Imran, M., Mativenga, P. T., Gholinia, A., & Withers, P. J. (2015)[28]	Inconel 718 alloy	Mechanical micro-drilling, electrical discharge machining and laser beam machining	Micro-drilling via mechanical methods presents enhanced mechanical, metallurgical, and geometrical characteristics when contrasted with laser and EDM techniques.
6	Singh, N., Talapatra, A., Junkaew, A., Duong, T., Gibbons, S., Li, & Arróyave, R. (2016)[31]	NiTi alloy	–	The effect of alloying on the thermodynamic and mechanical properties of B2 NiTi–X structures are presented.
7	Ahmet Balcı, Adem Çiçek, Necati Uçak, & Kubilay Aslantas. (2024)[32]	Ti6Al4V alloy	Conventional micro drilling and peck drilling	During the micro drilling higher thrust force, surface roughness, burr height, and tool wear were reported. The MQL condition significantly improved the hole quality during peck drilling. High speed machining found suitable for better hole quality.
8	Yunze Li, Zhijian Pei, Weilong Cong. (2025)[33]	Silicon	Conventional micro machining and rotary ultrasonic micro machining	A comparative study was conducted during the micro machining of silicon using conventional machining ang ultrasonic machining. Using ultrasonic machining reduces the thermal problems created by conventional machining. The hole quality is comparably high using ultrasonic machining. The paper also provides the mechanistic model for identifying relationship between parameters and hole quality.

Table 1. Glimpse of literatures available (indicatively) with respect to materials, and machining methods.

S. No	Element Name	Weight%
1	Nickel	51.8%
2	Titanium	46.38%
3	Carbon	0.052%
4	Cobalt	0.352%
5	Iron	0.18%
6	Other traces	Rem.

Table 2. Elemental weight% of the candidate material, low carbon NiTi alloy.

In addition to the research gaps mentioned above, there is a wide gap in the research articles containing carbon as an alloying element in NiTi binary system. Also, mostly the literatures have suggested that there is an increase in carbon percentage during EDM, the hole dimensions are not that controllable and uniform in LBM, and in both methods, the Heat Affected Zone (HAZ) is comparatively larger. From the existing research paradigm, it strongly supports the assertion that there is a demand for the study of drilling of low carbon NiTi alloy. The focal point of the research lies in the modified nickel-titanium alloy with a carbon element, which is subjected to machining studies. The principal intention of this research study is to perform micro-drilling on low-carbon NiTi alloy with 0.05% carbon utilizing tungsten carbide drills. Additionally, the objective is to comprehend the impact of feed rate and tool rotational speed on hole quality, machining time, and tool wear. The results are further elucidated with electron microscopic images and spectroscopic analyses for recommendations.

The novelty of this manuscript lies on the introducing the nickel -titanium alloy with an added element of carbon element (0.05%) and the levels of low rotational speed and feed rate. Very common smart materials possess nickel and titanium, however in this case the hardness of the material has been improved with addition of carbon element. The machining capability of the modified low carbon NiTi alloy is essential to witness the suitability of the material for several engineering applications.

Experimental procedure

Sample preparation

Nickel-titanium alloy, incorporating carbon as an alloying element, serves as the material employed in this study. The material composition is determined through optical emission spectroscopy, and the weight-based composition is presented in Table 2. The microstructure was unveiled using an optical microscope in conjunction with an appropriate metallurgical etchant, namely Beraha's Reagent, comprising 4 g NH_4SCN, 10 ml HCl, and 20

ml H_2O. The Carbon in the base material is recognized in the shape of spherical granules dispersed uniformly within the austenitic structure of the base material and the same depicted in Fig. 1.

Micro drilling

The metallurgically polished surface of the low carbon NiTi alloy is preserved as the cutting face for the investigation of micro-drilling using a tungsten carbide drill tool (diameter of 495 µm) in a cylindrical rod (diameter of 10 mm) to a thickness of 5 mm. Various cutting parameters are employed in the experimental design aimed at achieving micro-drilling with a diameter of 500 µm. The recommended machine tool for these experiments is the multipurpose micromachining centre (Make: MIKRO TOOLS, Singapore), equipped with an image analyser. The experiments involve maintaining a constant depth of cut (500 µm) while varying input process parameters within the ranges specified in Table 3. Nine different combinations of three levels of spindle

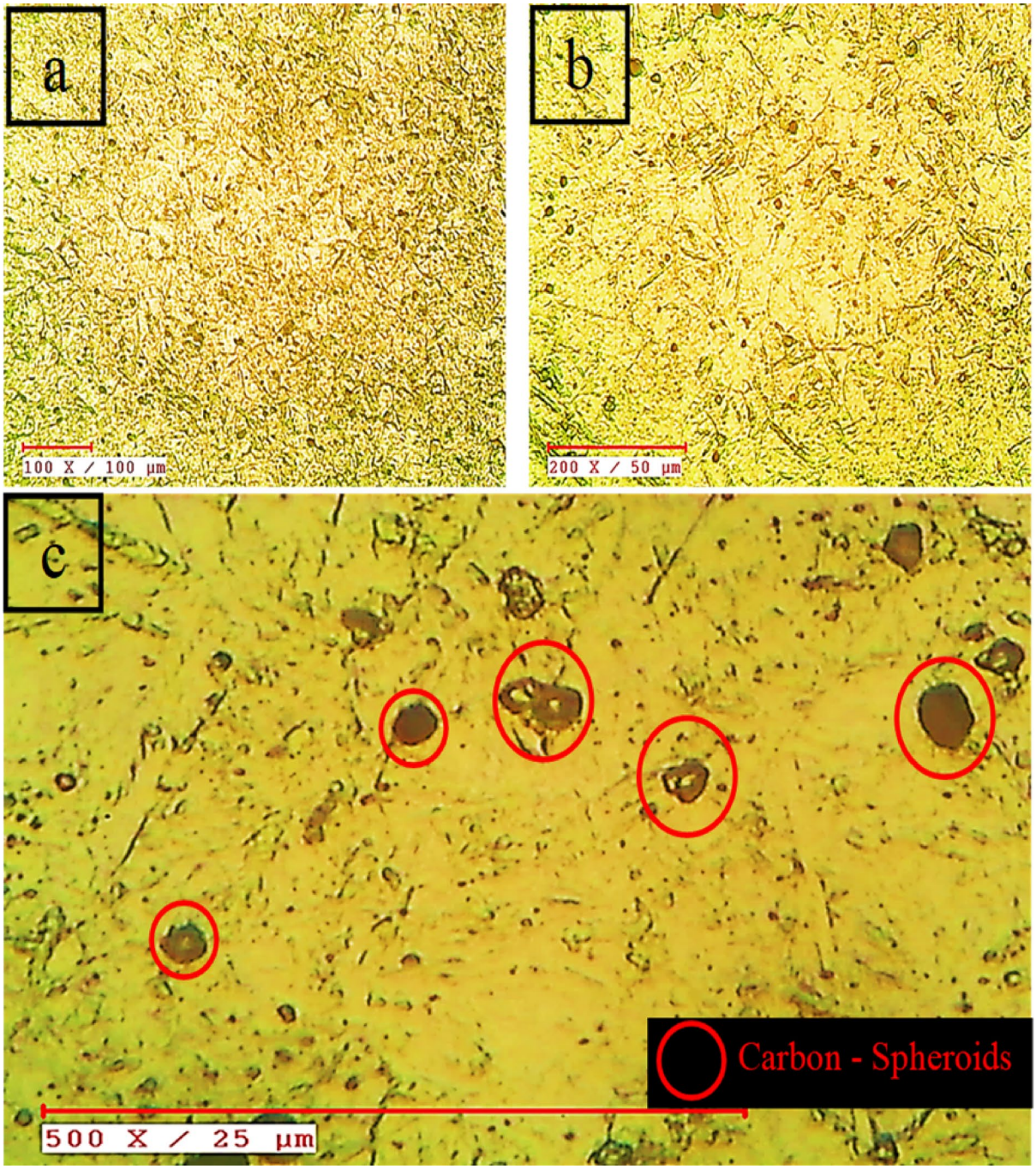

Fig. 1. Optical microscopic image of the low carbon NiTi alloy under different magnification showing spheroidal carbon granules.

Input Factors	Range	Unit
Tool Rotational speed	1500, 2000 and 2500	RPM
Feedrate	0.2, 0.4 and 0.6	mm/min
Length of cut	500	µm
Drill tool diameter	495	µm

Table 3. Range of input factors and their units.

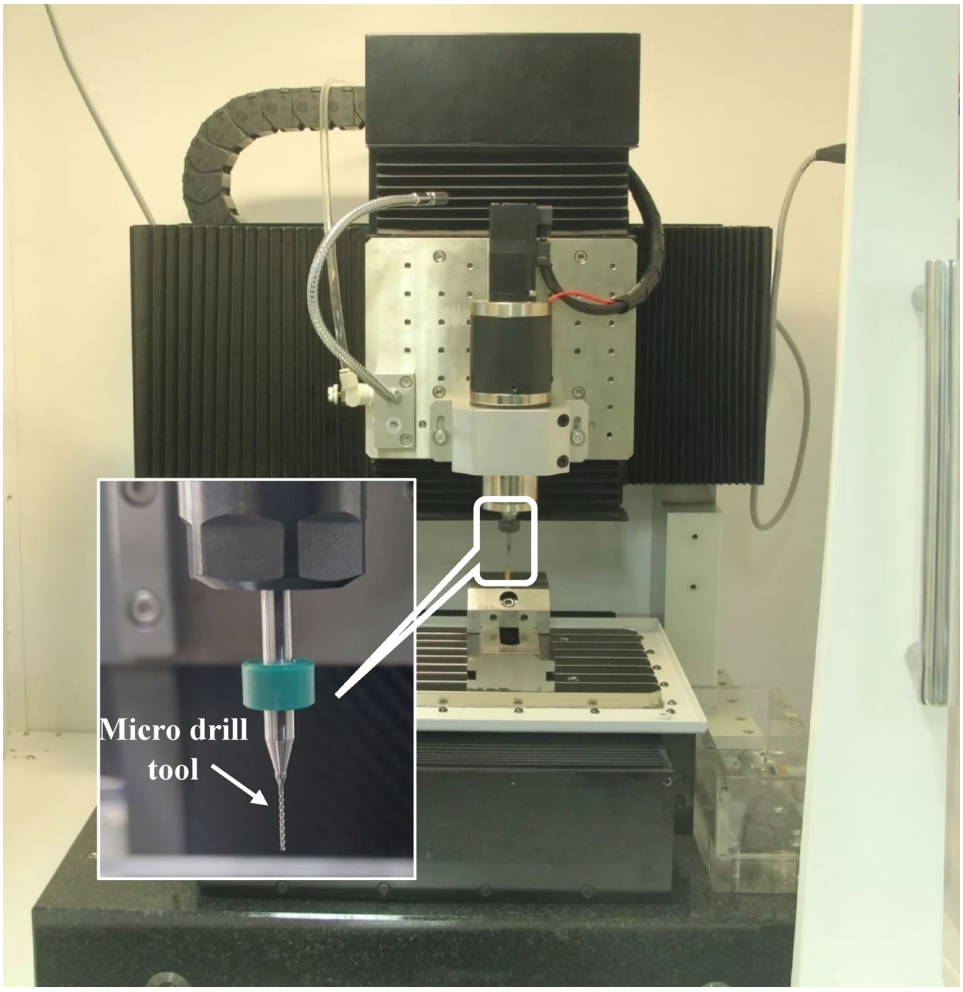

Fig. 2. Photographic image of the machining centre used for experimentation.

speed and tool feedrate are designed for the machining experiments. Figure 2 displays a photo image of the machining centre and the micro drill bit.

Throughout the machining process, the time taken for each experiment is measured and calculated. Following experimentation, the drill holes are examined using an optical microscope to assess the cylindricity of the machined layer for subsequent discussion. The scanning electron microscope is then employed to inspect the drill hole's open structure, shearing zone, and burr formation. Subsequent to this, an energy dispersive spectroscopic analysis is conducted on the micro-cutting tool. To examine the correlation between input process parameters and responses in micro-drill hole machining, Minitab® Statistical Software (v21.4) trial version (https://www.minitab.com/en-us/products/minitab-solution-center/free-trial/) is utilized.

Results and discussion

Micro drill hole diameter

A micro-drilling procedure with a diameter of 500 µm is executed on a low-carbon NiTi alloy using a tungsten carbide (WC) drill bit with a tool diameter of 495 µm. Following the machining process, a vertical microscope is employed to observe the micro-drills and measure the drill hole diameter. The average values of drill hole diameters are plotted against spindle speed for various feed rates, as illustrated in Fig. 3.

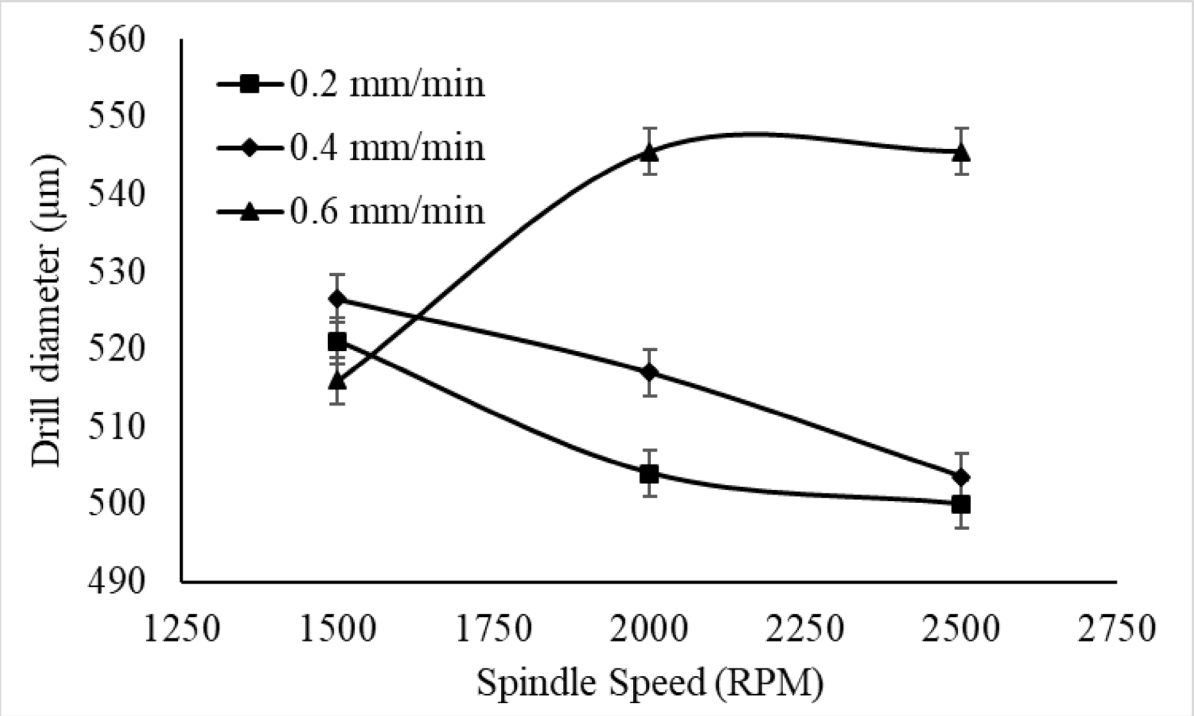

Fig. 3. Micro drill diameter (average value) measured with respect to different spindle speed.

Observations indicated that attaining a drill hole diameter close to the specified dimension (501 µm) was achieved during elevated drill rotational speed, 2500 RPM, with a minimal traverse feed of 0.2 mm/min. Conversely, maintaining the same drill rotational speed but increasing the traverse feed resulted in a proportional increase in drill hole diameter. Particularly, with a maximum traverse feed of 0.6 mm/min, the drill hole diameter peaked at an extreme dimension of 546 µm.

The observed increase in drill diameter is attributed to the elevated feed rate, aligning with findings in existing literature[1,13,34–38]. Elevated traverse feed rates impose significant force on the drill flute, leading to buckling and vibration during machining. As a consequence, deviations occur in the cutting axis, introducing nonlinearity in the drill hole and leading to diameter enlargement. These deviations can also trigger the creation of maximum shear zones and metallic burrs atop the drill hole, a phenomenon corroborated by prior studies[13,38–41].

At a tool rotational speed of 2000 RPM, the variation in size of drill hole was observed to be similar to that at 2500 RPM, with increases noted at higher traverse feed. Machining at slower speeds demonstrated disparities in drill hole size ranging from 516 µm to 527 µm. Figure 4 illustrates the influence of tool rotational speed and feed rate on micro drill hole accuracy, highlighting the significant role of traverse feed on drill hole diameter variability.

Specifically, at maximum feed rates, the interaction between the tool and the workpiece intensifies, leading to tool deviation from the axis and subsequent enlargement of the drill hole diameter. Feed rates ranging from 0.2 mm/min to 0.3 mm/min consistently yield exact drill hole size with minimum variation with the size of drill bit, particularly in high-speed machining scenarios. Decreases in tool rotational speed (< 2250 RPM) reveal noticeable eccentricities in drill hole diameter. Thus, slower rotational speeds can minimize error in micro drilling; however, maintaining a low traverse feed of 0.2 mm/min during high rotational speeds can achieve precise micro drilling without compromising quality. Additionally, examination of the micro drill hole using a field emission scanning electron microscope offers insights into accuracy and shear zone characteristics.

Electron microscopic metaphors are employed to assess the precision of micro-drill holes across three distinct ranges of input process parameters. In Fig. 5a, an accurate drill hole with a hole diameter of 501 µm is depicted, achieved under machining conditions of 2500 RPM and a traverse feed of 0.2 mm/min. As discussed in the diametrical study, the drill hole closely approaches the expected dimension of 500 µm, displaying minimal deviation during high- rotational speed of drill tool. At the near top edge of the drill hole, a thin metallic burr film is evident, reaching a maximum dimension of 15 µm to 20 µm. This phenomenon may be attributed to the adhesion or abrasion of thin metal chips generated during micro-machining. The findings are in agreement with Khan et al., where adhesion is the considered as a major wear mechanism during the deep hole drilling process[42]. Concurrently, at the blind end of the hole, an onion-like structure exit burr is observed, a result of the tool rotational speed of the drill tool. The formation of exit burrs are common during the micro drilling process, however, the formation of the burrs can be controlled by proper parameter selection[43].

For a drill hole having a nominal diameter of 516 µm, as presented in Fig. 5b illustrates the impact of a tool rotational speed of 2000 RPM and an increased traverse feed (0.4 mm/min), leading to shear and metal burr formation on the top surface. With rising feed rates, distortion becomes apparent on the drill hole's top

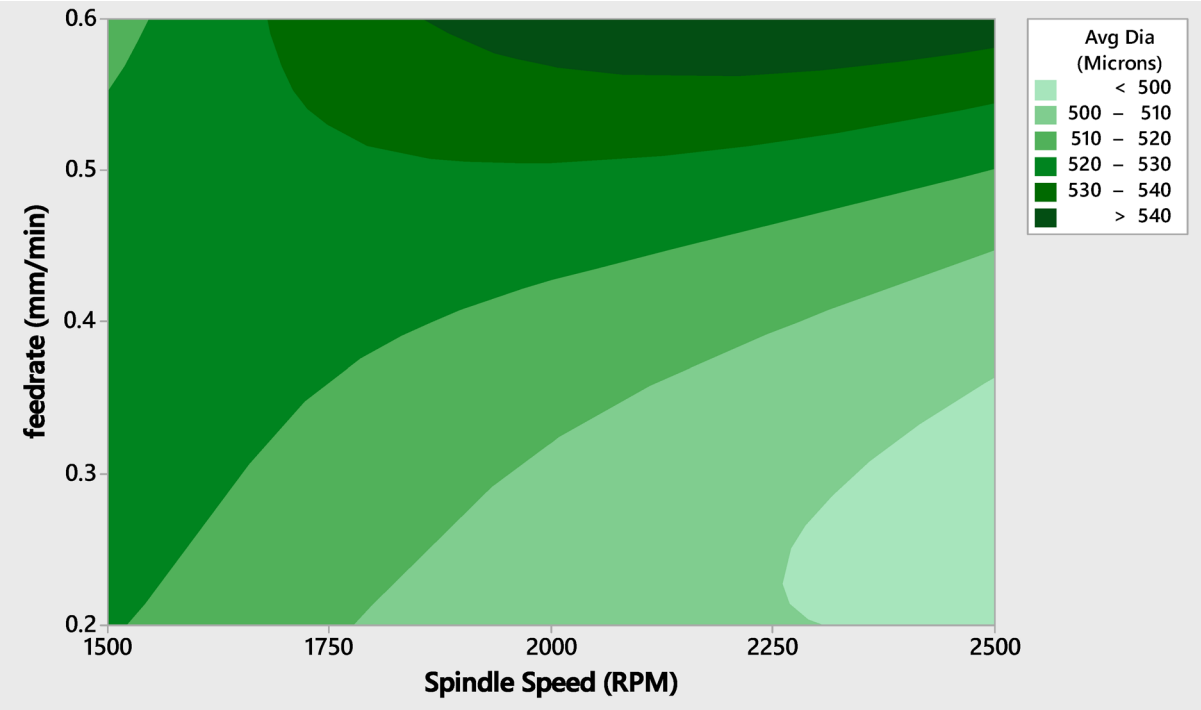

Fig. 4. Contour plot to indicate the accuracy in drill hole dimension with respect to tool rotational speed and feedrate.

surface. Utilizing Gwyddion software (v2.67–2024) (https://gwyddion.net/), dimensional changes are measured, revealing shear zone dimensions of 113 µm and 106 µm in the x- and y-coordinates, respectively.

Under the conditions of a tool rotational speed of 2500 RPM and a tool traverse feed of 0.6 mm/min, the drill hole diameter reaches a maximum of 546 µm. In this scenario, the x-coordinate exhibits a deviation of 178 µm, while the y-coordinate shows a deviation of 249 µm.

Expanding on the discussion regarding drill hole diameter, a noteworthy observation is the pronounced impact of an increased drill tool feed rate on the top surface, leading to significant material deformation and shear. Illustrated in Fig. 5c is the manifestation of metal shear on the top surface of the micro drill, specifically under the machining conditions of 2500 RPM rotational speed and a traverse feed of 0.6 mm/min. At this high tool rotational speed combined with the maximum traverse feed, the material exhibits a maximum shear zone, signifying extensive material deformation characterized by serrated metal chips along the edge of the drill hole.

Detailed electron images at higher magnification reveal the material deformation, evident in the form of shear, influencing the drill hole to present a wider surface at the top. The thrust force induced by the high feed rate contributes to material deformation, resulting in reduced shear but with the formation of sharp metal chips. Kim et al. found that the feed rate the major significant factor affecting the thrust force[44]. The significance is that while machining at high cutting speed the mechanical force induced the material to under maximum shear. The reflection of the shear at a particular region (especially at a micro level) strain hardening appears and brittle fracture appears. The outcome of the material fracture is clearly witnessed in the SEM image. This effect is mitigated by utilizing a minimum feed rate under the same high-speed machining conditions.

Machining time calculation

The calculation of machining time for micro drilling is carried out by measuring and applying Eq. 1. In Fig. 6a, the outcomes of the machining time calculation concerning input process parameters are presented. Notably, for a slow tool rotational speed, the maximum time to drill a 500 µm diameter at a depth of 500 µm with a documented time of 1.78 min. Conversely, a decreasing trend is noted, with an increase in both tool rotational speed and traverse feed rate during the cutting process. Specifically, a tool rotational speed of 2500 RPM combined with a feed rate of 0.6 mm/min results in a minimal micro-drilling time of 0.43 min. The reduction in micro-drilling time is a crucial factor for maximizing production rates.

In order to predict the machining time within the proposed design of experiments, a Gaussian elimination method is utilized to formulate a mathematical equation for evaluating and determining the machining time based on unknown parameters. The regression equation derived from the experimental design is presented in Eq. 2.

$$Machining\ Time\ (Tm) = \frac{length\ of\ drill\ hole}{tool\ rotational\ speed\ \times\ Traverse\ Feed}\ (\mathrm{min}) \tag{1}$$

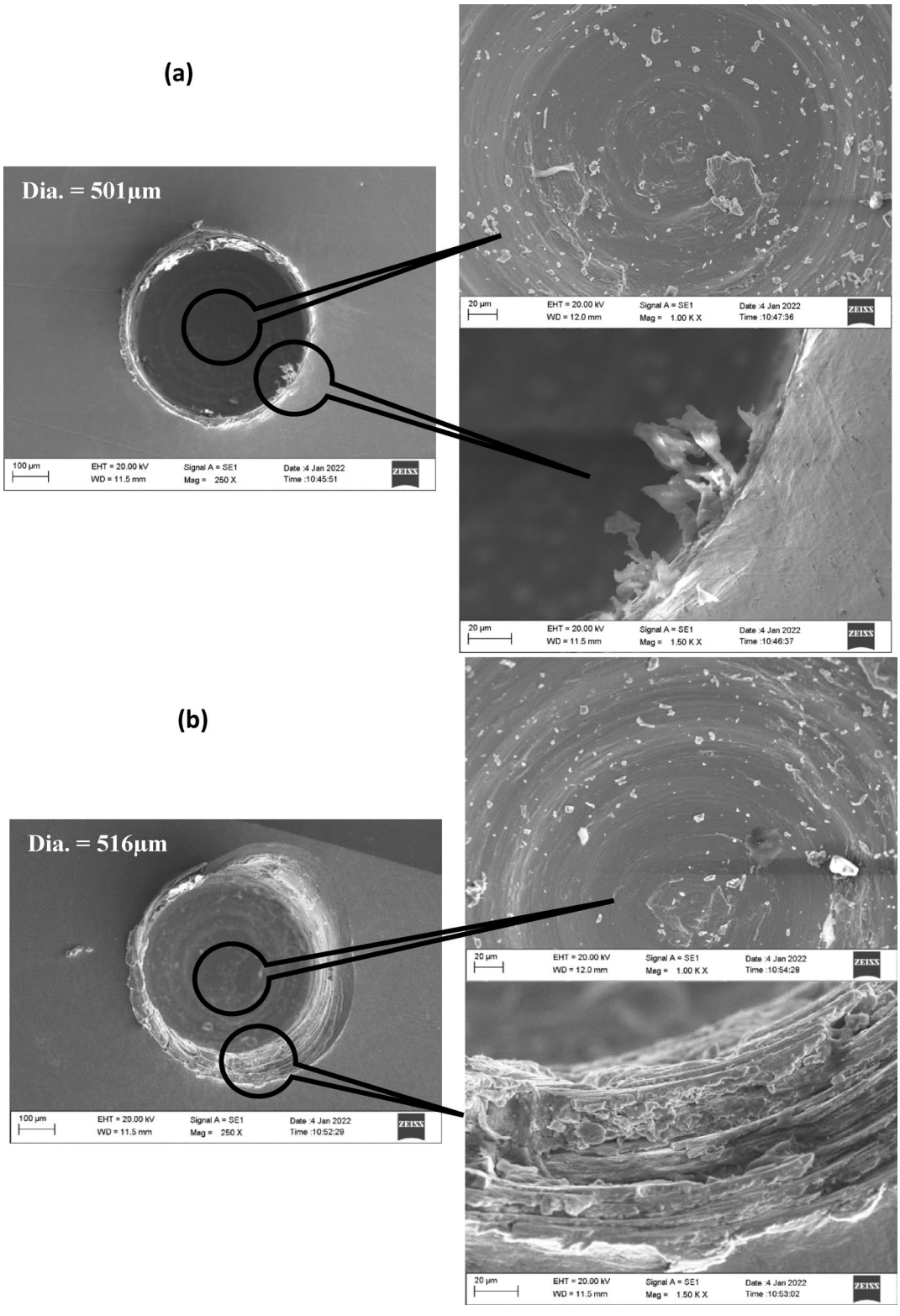

Fig. 5. **a** Perfect drill hole with a diameter of 501 µm, having burr and shear zone at the bottom of the blind hole. **b** Perfect drill hole with an average diameter of 516 µm, having metal shear zone at the start and end point of the blind hole. **c** Perfect drill hole with a maximum diameter of 546 µm, having metal shear zone the start and end point of the blind hole.

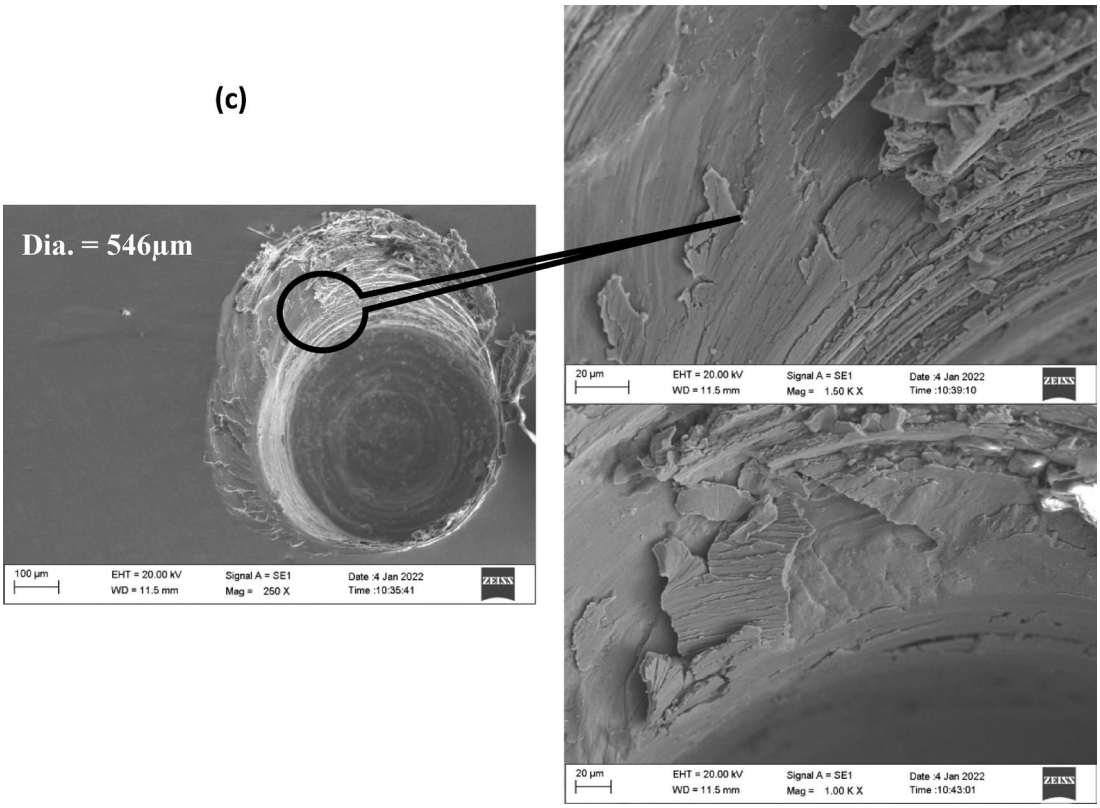

Fig. 5. (continued)

$$Machining\ Time\ (Tm) = 136.121\ S^{-0.803}\ f^{-0.928}\ (\min) \tag{2}$$

where, S - tool rotational speed F – Traverse Feed.

Figure 6b presents the anticipated machining time, as determined by the regression equation derived through Gaussian elimination. Calculations were performed for specific input factors, such as tool rotational speed and traverse feedrate, based on the regression equation for comparison. The graph (Fig. 6c) illustrates that the variance between the initial values and the machining time derived from regression is minimal and negotiable. Each point on the graph closely aligns, and the regression line, representing machining time, closely follows the path of the initially measured line.

For a more detailed analysis, the relationship between machining time, spindle speed, and feedrate is depicted in a contour plot, showcased in Fig. 7. The optimal conditions for minimizing machining time are achieved at maximum tool rotational speed and traverse feedrate. However, the range of input parameters is substantial, spanning from 1900 RPM to 2500 RPM for tool rotational speed and from 0.45 mm/min to 0.6 mm/min for feedrate. To enhance comprehension, the optimal process conditions are expected to fall within the specified range of process parameters.

Tool wear analysis

Figure 8 displays a scanning electron microscopic image depicting the tungsten carbide (WC) micro drill tool bit following the machining of low-carbon NiTi alloy at 2500 RPM with a feed rate of 0.2 mm/min. Initially, the diameter of the WC micro drill tool is 495 µm. After machining for 1.2 min, wear on the tool is evident, resulting in a reduced diameter of 492.2 µm. Notably, significant deformation is observed on the cutting nose of the drill tool, which is attributed to friction encountered during machining the low-carbon NiTi alloy.

The micro hardness of the utilized low-carbon NiTi alloy is measured at 341 Hv, while the micro hardness of the WC micro drill bit is recorded as 639 Hv. This discrepancy in hardness values suggests that the chosen cutting tool effectively facilitated the subtraction of material from the low-carbon NiTi alloy with a trifling wear rate.

Examining the cutting edge of the micro drill bit at a higher magnification of 1500X reveals tool wear in the form of abrasion at the chisel (tool nose) and adhesive on the flute of the micro drill tool bit (refer to Fig. 9). Specifically, the measured tool wear at the cutting tool nose is 22 µm, representing abrasion. The rate of abrasion is minimal, given that the hardness of the WC micro drill bit is twice that of the work material. Furthermore, the cutting-edge profile exhibits sharpness and minute dimensions. Consequently, due to the tool nomenclature and the material characteristics of the cutting tool, the occurrence of tool failure is minimal and deemed acceptable for continuous machining.

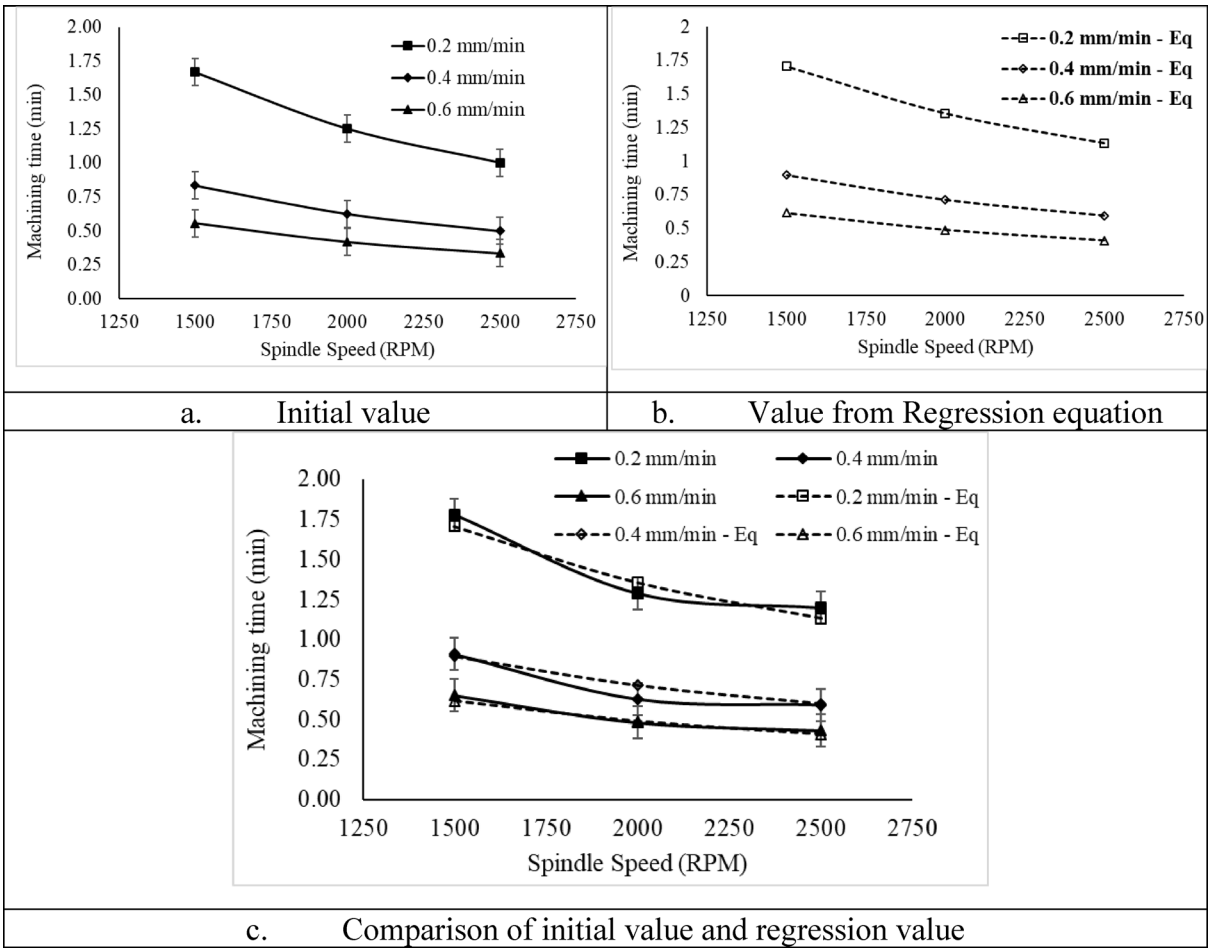

Fig. 6. Comparison of machining time with initial and regression value.

In addition to abrasive tool wear, material from the workpiece, deformed during micro-drilling, adheres to the drill flute due to the frictional force generated during high spindle speed, as depicted in Fig. 9. Complementing the evaluation of tool wear, an energy dispersive spectroscopic analysis is conducted on the worn tool. The spectroscopic results indicate that abrasive wear predominantly comprises the tool bit material, with tungsten and carbide identified as major alloying elements (see Fig. 10a). Furthermore, alloying elements from the work material are observed at the tool edge, albeit with a minor contribution.

Subsequently, an investigation into the flute with adhesive wear on the drill tool bit reveals major alloying elements such as C, O, Ni, and Ti at the tool edge (refer to Fig. 10b). Therefore, the tungsten carbide (WC) base cutting tool stands out as one of the commercially available cutting tools in the market, suitable for machining low-carbon NiTi alloy under optimal machining parameters.

Conclusions

This work introduces optimized procedure to produce micro-sized holes through high-speed machining of low-carbon NiTi alloy using a WC drill tool, and the following points are concluded.

1. High drill tool rotational speed of 2500 RPM proves to be a valid parameter for achieving a drill hole average diameter of 501 µm, closely matching the design diameter of 500 µm. This successful outcome was obtained with a minimal traverse feed of 0.2 mm/min. However, when the traverse feed was elevated to 0.6 mm/min while maintaining the same drill rotational speed, the drill hole diameter increased to 546 µm.
2. The notable variations in the drill hole diameter can be attributed to dynamic fluctuations occurring in the drill tool, manifesting as tool buckling and outing. The thrust force and fluctuations in the WC drill bit contribute significantly to wear on the cutting edge. Consequently, the drill opening diameter experiences maximum shear and material deformation, leading to phenomena such as chip formation and the development of burrs at the top of the drill hole.
3. During the cutting process, the material undergoes shear and adheres along the path of the drill flute. The elasticity of the low-carbon NiTi alloy increases as a result of microchipping in shear form. In this phase, the deformed material slides along the drill flutes and attaches in the shape of a continuous ribbon over the cutting edges.

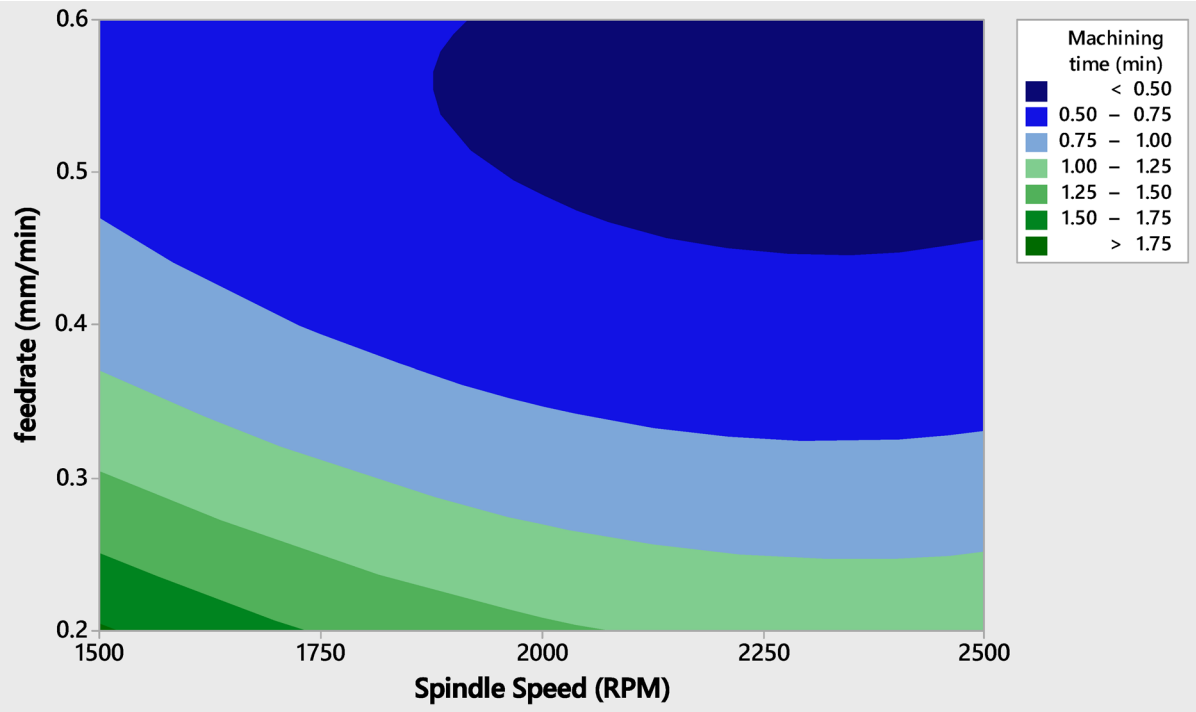

Fig. 7. Contour plot to indicate the machining time performed on micro drilling on low carbon NiTi alloy with respect to tool rotational speed and traverse feedrate.

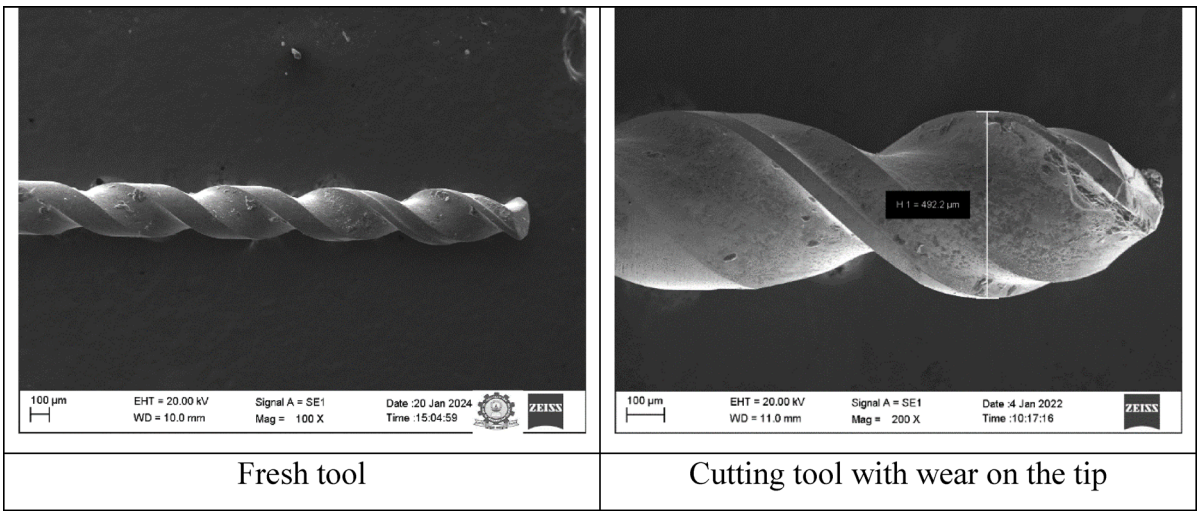

Fig. 8. Scanning electron microscopic image showcasing the diameter (492.2 µm) of the micro drill tool after the machining operation.

4. High-speed machining is justified, as it allows the tool to achieve the defined tool path efficiently. The minimum machining time is documented as 0.43 min for a combination of 2500 RPM and 0.6 mm/min, and 1.78 min for 1500 RPM with 0.2 mm/min, respectively. When comparing the performance of micro drilling in terms of drill hole diameter and machining time, it is advisable to opt for high-speed machining when working on low carbon NiTi alloy using a WC drill tool.

In summary, it is advisable to utilize the WC micro drill tool with a high tool rotational speed and low traverse feed rate, as it exhibits improved machinability and accuracy.

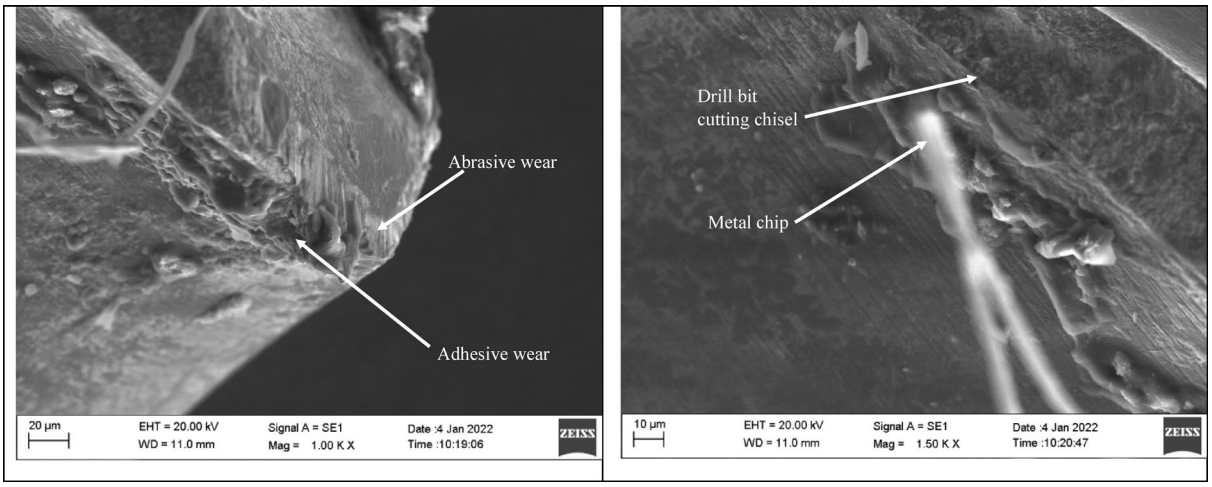

Fig. 9. Scanning electron microscopic image of worn-out tool used to show the tool wear and adhesion of metal chips at the cutting edge.

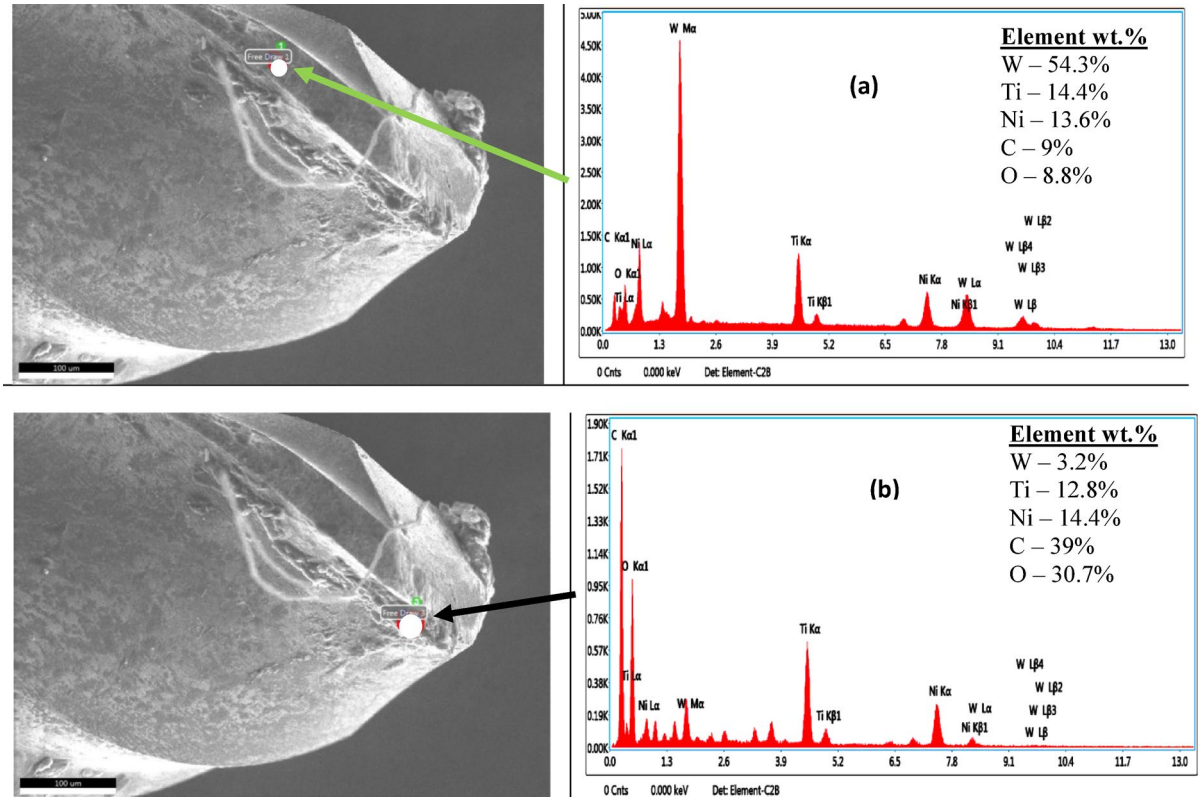

Fig. 10. **a** EDS result on cutting tool chisel indicating abrasion in the tool surface along with scanning electron microscopic image. **b** EDS result on cutting tool chisel indicating the presence of workpiece material on the tool edge along with scanning electron microscopic image.

Scope for future work

This work presented a practical approach to micro drill low carbon NiTi alloy under different speeds and feeds for understanding the betterment of the process by measuring the quality of hole, wear on tool surface and material removal rate.

This work can be further improved by comparing the various percentage of the carbon as ternary compound in the NiTi binary system. This might explore the upshot of the carbon content in the quality of the micro drilling process.

The NiTiC alloy manufactured by means of the 3D printing can be explored for the stability and quality of the material for various percentages if the carbon.

The quaternary effect of the NiTi is booming but still the research is restricted to hafnium, zirconium, niobium, etc., still there are possibilities to explore the combination of carbon as the quaternary element.

The hybrid sequential micro drilling is emerging, but not on the NiTiC combinations, it can be explored.

Data availability

The data will be shared to the readers based on the request by the corresponding author.

Received: 17 July 2025; Accepted: 9 October 2025
Published online: 17 November 2025

References

1. Geier, N. et al. A critical review on mechanical micro-drilling of glass and carbon fibre reinforced polymer (GFRP and CFRP) composites, compos. *Part. B Eng.* **254**, 110589. https://doi.org/10.1016/j.compositesb.2023.110589 (2023).
2. Chaudhari, R., Vora, J. J., Patel, V., López de Lacalle, L. N. & Parikh, D. M. Surface Analysis of Wire-Electrical-Discharge-Machining-Processed Shape-*Memory Alloys Mater.* **13** (2020) 530. https://doi.org/10.3390/ma13030530.
3. Agrawal, V., Gajrani, K. K., Mote, R. G., Barshilia, H. C. & Joshi, S. S. Wear analysis and tool life modeling in micro drilling of Inconel 718 superalloy. *J. Tribol* https://doi.org/10.1115/1.4054294 (2022).
4. Manjaiah, M., Narendranath, S. & Basavarajappa, S. Review on non-conventional machining of shape memory alloys. *Trans. Nonferrous Met. Soc. China*. **24**, 12–21. https://doi.org/10.1016/S1003-6326(14)63022-3 (2014).
5. Takale, A. M. & Chougule, N. K. Effect of wire electro discharge machining process parameters on surface integrity of Ti49.4Ni50.6 shape memory alloy for orthopedic implant application. *Mater. Sci. Eng. C Mater. Biol. Appl.* **97**, 264–274. https://doi.org/10.1016/j.msec.2018.12.029 (2019).
6. Ou, S. F., Peng, B. Y., Chen, Y. C. & Tsai, M. H. Manufacturing and characterization of NiTi alloy with functional properties by selective laser melting. *Metals* **8**, 342. https://doi.org/10.3390/met8050342 (2018).
7. Sonawane, S. A. & Kulkarni, M. L. Optimization of machining parameters of WEDM for Nimonic-75 alloy using principal component analysis integrated with Taguchi method. *J. King Saud Univ. - Eng. Sci.* **30**, 250–258. https://doi.org/10.1016/j.jksues.2018.04.001 (2018).
8. Kumar, S., Batish, A., Singh, R. & Bhattacharya, A. Effect of cryogenically treated copper-tungsten electrode on tool wear rate during electro-discharge machining of Ti-5Al-2.5Sn alloy. *Wear* **386–387**, 223–229. https://doi.org/10.1016/j.wear.2017.01.067 (2017).
9. Soni, H., Narendranath, S. & Ramesh, M. R. Experimental investigation on effects of wire electro discharge machining of Ti50Ni45Co5 shape memory alloys. *Silicon* **10**, 2483–2490. https://doi.org/10.1007/s12633-018-9780-9 (2018).
10. Soni, H., Sannayellappa, N. & Rangarasaiah, R. M. An experimental study of influence of wire electro discharge machining parameters on surface integrity of TiNiCo shape memory alloy. *J. Mater. Res.* **32**, 3100–3108. https://doi.org/10.1557/jmr.2017.137 (2017).
11. Mouralova, K. et al. Precision machining of nimonic C 263 super alloy using WEDM. *Coatings* **10**, 590. https://doi.org/10.3390/coatings10060590 (2020).
12. Szwajka, K., Zielińska-Szwajka, J., Żaba, K. & Trzepieciński, T. An investigation of the sequential Micro-Laser drilling and conventional Re-Drilling of Angled holes in an inconel 625 Ni-Based alloy. *Lubricants* **11**, 384. https://doi.org/10.3390/lubricants11090384 (2023).
13. Shukla, S., Jain, R. & Gangopadhyay, S. Measurement and analysis of radial force, radial torque and surface integrity in micro-drilling of an Al7075-T6 alloy. *Proc. Inst. Mech. Eng. Part B J. Eng. Manuf.* **238**, 1183–1195. https://doi.org/10.1177/09544054231189104 (2024).
14. Kaya, E. & Kaya, İ. Investigation of high speed cutting performance and phase transformation behavior of NiTi shape memory alloys. *Int. J. Adv. Manuf. Technol.* **119**, 489–502. https://doi.org/10.1007/s00170-021-08254-1 (2022).
15. Kumar, V., Sharma, N., Kumar, K. & Khanna, R. Surface modification of WC-Co alloy using Al and Si powder through WEDM: A thermal erosion process. *Part. Sci. Technol.* https://doi.org/10.1080/02726351.2017.1317308 (2018).
16. Islam, A. & Dwivedi, V. K. An experimental study on major process parameters effecting the type of burrs in drilling operation for mild steel ASTM A-36. In *Addit. Subtractive Hybrid Technol. Recent Innov. Manuf* (eds Prakash, C. et al.) 13–40 (Springer International Publishing, 2022). https://doi.org/10.1007/978-3-030-99569-0_2.
17. Kuppuswamy, R. & Yui, A. High-speed micromachining characteristics for the NiTi shape memory alloys. *Int. J. Adv. Manuf. Technol.* **93**, 11–21. https://doi.org/10.1007/s00170-015-7598-9 (2017).
18. Patra, K., Jha, A. K., Szalay, T., Ranjan, J. & Monostori, L. Artificial neural network based tool condition monitoring in micro mechanical Peck drilling using thrust force signals. *Precis Eng.* **48**, 279–291. https://doi.org/10.1016/j.precisioneng.2016.12.011 (2017).
19. Anand, R. S., Patra, K., Steiner, M. & Biermann, D. Mechanistic modeling of micro-drilling cutting forces. *Int. J. Adv. Manuf. Technol.* **88**, 241–254. https://doi.org/10.1007/s00170-016-8632-2 (2017).
20. Azim, S., Gangopadhyay, S., Mahapatra, S. S., Mittal, R. K. & Singh, R. K. Role of PVD coating on wear and surface integrity during environment-friendly micro-drilling of Ni-based Superalloy. *J. Clean. Prod.* **272**, 122741. https://doi.org/10.1016/j.jclepro.2020.122741 (2020).
21. Shrivastava, A. & Gangopadhyay, S. Evaluation of adequacy of lubricants in MQL micro-drilling by a developed analytical model and experiments. *J. Manuf. Process.* **101**, 1592–1604. https://doi.org/10.1016/j.jmapro.2023.07.017 (2023).
22. Abbas, A. T. et al. Towards optimization of surface roughness and productivity aspects during high-speed machining of Ti–6Al–4V. *Materials* https://doi.org/10.3390/ma12223749 (2019).
23. Sharma, N., Gupta, K. & Davim, J. P. On wire spark erosion machining induced surface integrity of Ni55.8Ti shape memory alloys. *Arch. Civ. Mech. Eng.* **19**, 680–693. https://doi.org/10.1016/j.acme.2019.02.004 (2019).
24. Ashwinkumar Hegde, K. R., Talla, G. & Gangopadhyay, S. Tool condition monitoring and hole quality analysis during micro-drilling of NiTi shape memory alloy using artificial neural network. *Measurement* **253**, 117487. https://doi.org/10.1016/j.measurement.2025.117487 (2025).
25. Chaudhary, K., Haribhakta, V. K. & Kanake, V. Optimization of hole quality in micro-drilling of nitinol - Using box-Behnken surface methodology (RSM) design. *Results Eng.* **27**, 105699. https://doi.org/10.1016/j.rineng.2025.105699 (2025).
26. Matta, C. S. K., Talla, G., Hegde, K. R. A. & Gangopadhyay, S. Effect of radial force and radial torque on hole quality characteristics during Micro-Drilling of nitinol shape memory alloy. *Int. J. Precis Eng. Manuf.* **26**, 1131–1140. https://doi.org/10.1007/s12541-024-01186-2 (2025).
27. Sethi, A., Acharya, B. R. & Saha, P. Parametric investigation of pulse frequency and microtool rotational speed for precise fabrication of microchannels on nitinol shape memory alloy through ECMM. *Mater. Today Commun.* **36**, 106844. https://doi.org/10.1016/j.mtcomm.2023.106844 (2023).

28. Imran, M., Mativenga, P. T., Gholinia, A. & Withers, P. J. Assessment of surface integrity of Ni Superalloy after electrical-discharge, laser and mechanical micro-drilling processes. *Int. J. Adv. Manuf. Technol.* **79**, 1303–1311. https://doi.org/10.1007/s00170-015-6909-5 (2015).
29. Prashanth, P. & Hiremath, S. S. Experimental and predictive modelling in dry micro-drilling of titanium alloy using Ti–Al–N coated carbide tools. *Int. J. Interact. Des. Manuf. IJIDeM*. **17**, 553–577. https://doi.org/10.1007/s12008-022-01032-7 (2023).
30. Kundiya, R. et al. Analysis of Hole Characteristics in Mechanical Micro-drilling of CFRP-Ti6AI4V Stack Composite. In *Adv. Mater. Agile Manuf.* (eds Kumar, N. et al.) 37–51 (Springer, 2024). https://doi.org/10.1007/978-981-99-6601-1_5.
31. Singh, N. et al. Effect of ternary additions to structural properties of NiTi alloys. *Comput. Mater. Sci.* **112**, 347–355. https://doi.org/10.1016/j.commatsci.2015.10.029 (2016).
32. Balcı, A., Çiçek, A., Uçak, N. & Aslantas, K. Investigation of the effects of heat treatment and hot isostatic pressing in micro-drilling of Ti6Al4V alloy fabricated by laser powder bed fusion. *Precis Eng.* **91**, 617–631. https://doi.org/10.1016/j.precisioneng.2024.10.016 (2024).
33. Li, Y., Pei, Z. & Cong, W. Parametric and theoretical study of hole quality in conventional micro-machining and rotary ultrasonic micro-machining of silicon. *Precis Eng.* **93**, 167–176. https://doi.org/10.1016/j.precisioneng.2025.01.008 (2025).
34. Khadtare, A. N., Pawade, R. & Joshi, S. S. Experimental study in Micro-drilling mechanism on heterogeneous structure of thermal barrier coated inconel 718 Superalloy. *Int. J. Precis Eng. Manuf.* **25**, 509–525. https://doi.org/10.1007/s12541-023-00909-1 (2024).
35. Balázs, B. Z., Geier, N., Takács, M. & Davim, J. P. A review on micro-milling: recent advances and future trends. *Int. J. Adv. Manuf. Technol.* **112**, 655–684. https://doi.org/10.1007/s00170-020-06445-w (2021).
36. Wu, Z., Zhang, F. & Feng, K. Simulation analysis of titanium alloy micro-drilling based on thermo-mechanical coupling. *J. Phys. Conf. Ser.* **2338**, 012067. https://doi.org/10.1088/1742-6596/2338/1/012067 (2022).
37. Zhao, S., Bai, X., Xu, D. & Cao, W. Effects and mechanism of Micro-Drilling parameters on the drilling force and hole morphology of Sapindus mukorossi seeds. *Forests* **14**, 1162. https://doi.org/10.3390/f14061162 (2023).
38. Yalçın, B., Yüksel, A., Aslantaş, K., Der, O. & Ercetin, A. Optimization of Micro-Drilling of laminated aluminum composite panel (Al–PE) using Taguchi orthogonal array design. *Materials* **16**, 4528. https://doi.org/10.3390/ma16134528 (2023).
39. Joshy, J. & Kuriachen, B. Influence of post-processing and build orientation on the micro-machinability and chip formation during micro-drilling of L-PBF AlSi10Mg. *CIRP J. Manuf. Sci. Technol.* **45**, 35–48. https://doi.org/10.1016/j.cirpj.2023.05.009 (2023).
40. Zannoun, H. & Schoop, J. Analysis of burr formation in finish machining of nickel-based Superalloy with worn tools using micro-scale in-situ techniques. *Int. J. Mach. Tools Manuf.* **189**, 104030. https://doi.org/10.1016/j.ijmachtools.2023.104030 (2023).
41. Gao, G., Sun, Z., Pan, X., Li, J. & Xiang, D. Study of longitudinal-torsional ultrasonic-assisted vibration on micro-hole drilling Zr-based metallic glass. *Int. J. Adv. Manuf. Technol.* **131**, 2893–2907. https://doi.org/10.1007/s00170-023-12649-7 (2024).
42. Khan, S. A. et al. Deep hole drilling of AISI 1045 via high-speed steel twist drills: evaluation of tool wear and hole quality. *Int. J. Adv. Manuf. Technol.* **93**, 1115–1125. https://doi.org/10.1007/s00170-017-0587-4 (2017).
43. Ahn, Y. & Lee, S. H. Classification and prediction of burr formation in micro drilling of ductile metals. *Int. J. Prod. Res.* https://doi.org/10.1080/00207543.2016.1254355 (2017).
44. Kim, D. W., Cho, M. W., Seo, T. & Lee, E. S. Application of design of experiment method for thrust force minimization in Step-feed micro drilling. *Sensors* **8**, 211–221. https://doi.org/10.3390/s8010211 (2008).

Acknowledgements

The authors express their gratitude to UAE University and Sultan Qaboos University for the generous provision of resources and financial support via joint Fund (#12N271).

Author contributions

A.K.M and A.H.I.M conceptualized the idea. A.K.M and E.G wrote the methodology and testing. E.G wrote the manuscript draft. W.J.JT and D.T.T verified the test data. A.K.M and A.H.I.M performed supervision. A.H.I.M received the funding. All authors reviewed the manuscript.

Funding

The authors express their gratitude to UAE University and Sultan Qaboos University for the generous provision of resources and financial support via joint Fund (#12N271).

Declarations

Competing interests

The authors declare no competing interests.

Additional information

Correspondence and requests for materials should be addressed to A.-H.M.

Reprints and permissions information is available at www.nature.com/reprints.

Publisher's note Springer Nature remains neutral with regard to jurisdictional claims in published maps and institutional affiliations.